

## OPTIMIZATION OF ION SOURCE EXTRACTION AND TRANSPORT WITH SYMBOLIC MANIPULATION PROGRAMS: ELECTROSTATIC LENSES FORMULAS

M. Cavenago

INFN-LNL, via Romea n 4 I-35020 Legnaro (PD) Italy

### Abstract

The partly built line of the ECR ion source Alice, mainly based on electrostatic elements, needs several optimizations for different ion beam ( $A/q$  ranges from 2 to 9). Numerical codes easy to maintain and fast to execute were in demand. Beam optics codes are usually implemented as a kind of object oriented programs followed by a purposely written high level interpreter. This level was here replaced by general programs, combining symbolic and numerical capability, which therefore support different programming styles and a much finer physical description. Highly efficient linear tracking of electrostatic elements was obtained combining piecewise analytical solutions for quadratic and linear elements; some basic formulas and a sample result for Alice line are shown. Extension of elements to nonlinear case is given here, with detail for the anode lens.

### Introduction

The beam transport system of the ECR [1] ion source Alice is mainly constituted by electrostatic elements (extractor, three einzel lens and the accelerating column), with one magnetic dipole for charge selection (Fig. 1). Due to the relative importance of fringing fields, our need for a flexible and easily adaptable matrix tracking code was apparent; nonlinear effects were also considered a second goal. We wrote some application programs, executed (interactively) by Mathematica [2]. Usual formulas for sources, drifts, thin lens and dipoles were easily implemented, as well as graphic capabilities. This paper describes the nontrivial approximations and equations that we used in simulating round electrostatic elements in some detail.

Paraxial analysis of einzel lens was indeed possible, by decomposing the lens in seven regions (or elements), where the axial field  $E_z$  is assumed either constant (linear elements) or linearly increasing (quadratic elements) [3]. Use of more than three regions allows a closer fit to actual fields. A noteworthy nonlinear approximation (nonlinear means applicable to nonparaxial rays), namely the Piecewise Quadratic Approximation (PQA) is first introduced and briefly discussed; matching between linear and quadratic element is extended off-axis, allowing region boundaries to make a  $\arctg\sqrt{2}$  angle with  $z$  axis and introducing fictitious charges on element boundaries. We apply this general concept to anode lens effect.

We follow SI units in the code (generally) and use nonrelativistic mechanics, as suitable for ion sources. Since orbits do not depend on mass and charge in electrostatic fields, in section 2 and 3 we set unit mass and charge  $e = m = 1$  for brevity.

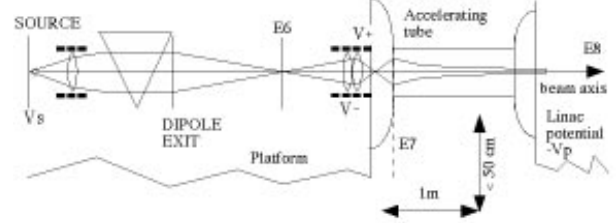


Figure 1: Beam line from platform (scale is approximated; transverse dimension exaggerated).

### Einzel Lens Paraxial Model

Let  $E$  be the total particle energy, a constant of motion, valid for every element of our beamline. First, we review the quadratic element. Consider a vacuum region where the electrostatic potential  $\phi(r, z)$  is exactly:

$$\phi(r, z) = A + Bz + C\left(\frac{1}{4}r^2 - \frac{1}{2}z^2\right) \quad (1)$$

Hamiltonian separates as  $H = H_z + H_r$  with  $H_r = (2p_r^2 + Cr^2)/4$ , whose value  $H_r^c$  is a constant of motion; also the value of  $H_z$  is the constant of motion  $H_z^c = E - H_r^c$ . Solving motion equations and eliminating  $t$  in favour of  $z$  we write the motion from  $z_i$  to  $z_o$  as

$$\begin{pmatrix} r \\ p_r \end{pmatrix}_o = \begin{pmatrix} \cos \psi & \sqrt{2/C} \sin \psi \\ -\sqrt{C/2} \sin \psi & \cos \psi \end{pmatrix} \begin{pmatrix} r \\ p_r \end{pmatrix}_i \quad (2)$$

$$\psi(z_o, z_i) = \frac{1}{\sqrt{2}} \text{Arsh} \left[ \frac{Cz - B}{\sqrt{2H_z^c C - 2AC - B^2}} \right]_{z_i}^{z_o} \quad (3)$$

with  $2H_z^c = 2E - p_r^2(z_i) - Cr^2(z_i)/2$ . From these nonlinear formulas a linear approximation in  $(r, p_r)$  is obtained by putting  $H_z^c = E$  in eq. (3). In case  $C < 0$  analytic continuation is taken. Case  $C = 0$  is the linear element.

The potential of einzel lens  $\Phi(r, z)$  can be fitted by elements like eq. (1) on intervals of  $z$  axis  $r = 0$ ; interval borders  $z_n$  are called breaking points here. In present code, we find convenient to use the well-known approximation for symmetrical einzel lenses [3]:

$$\Phi(0, z) = \frac{V_2}{2\omega(z_b - z_a)} \log \frac{\text{ch}[\omega(z + z_b)]\text{ch}[\omega(z - z_b)]}{\text{ch}[\omega(z + z_a)]\text{ch}[\omega(z - z_a)]} \quad (4)$$

with  $\omega = 1.318/R$  where  $R$  is the radius of electrodes and  $z = z_a, z = z_b$  their faces; in perspective, also the potential

$\Phi(0, z)$  numerically computed (by POISSON) and adequately interpolated can be fitted by the same elements.

Elements are easily counted by plotting (see Fig. 2a) the second derivative  $\Phi_{,zz}$  and associating a  $C > 0$  element to some maximum (region III) and a  $C < 0$  element to some minimum (region I) or low plateau. Between these elements, a  $C = 0$  element (region II) will certainly improve matching. At  $z = 0$  we can include a  $C = B = 0$  element (region 0) or not, depending on lens dimension  $z_a$ . In these regions, potential elements on axis are better written:

$$\begin{aligned} \phi &= a & 0 < z < z_0 \\ \phi &= a + \frac{1}{2}b(z - z_0)^2 & z_0 < z < z_1 \\ \phi &= c + d(z - z_0) & z_1 < z < z_2 \\ \phi &= \frac{1}{2}e(z - z_3)^2 & z_2 < z < z_3 \end{aligned} \quad (5)$$

and  $\phi = 0$  for  $z > z_3$ . Imposing continuity of  $\phi(0, z)$  and  $\phi_{,z}(0, z)$  everywhere, we get  $c = a - \frac{1}{2}d(z_1 - z_0)$ ,  $e = d/(z_2 - z_3)$  and  $z_3 = -2(a/d) + z_0 + z_1 - z_2$ .

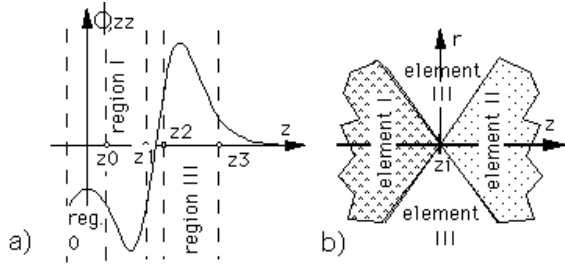


Figure 2: a) Breaking point determination from potential derivatives on  $z$  axis; 2b) Regions at a breaking point.

We choose  $a = \Phi(0, 0)$  to exactly reproduce the field at lens middle. The remaining parameter  $z_0, z_1, z_2$  (breaking points) and  $d$  can be determined by fitting  $\phi$  to the actual potential  $\Phi$ , that is by minimizing the norm

$$\sum_{z^{(j)}} w_0(\phi - \Phi)^2 + w_1(\phi_{,z} - \Phi_{,z})^2 + w_2(\phi_{,zz} - \Phi_{,zz})^2 \quad (6)$$

where  $z^{(j)} = j(L/N)$  and  $L$  is long enough ( $L = z_b + 3R$  suffices). Considering also the second derivative is essential for sound results of the fit, even if weights  $w_0, w_1$  and  $w_2 \neq 0$  may be varied; we choose  $w_n = R^n$ . Note that  $x_0 \leq 0$  is our criterion to drop region 0, which case leaves five intervals in total instead of seven.

In the paraxial approximation we can take region boundaries as  $z = z_n$  planes, and extend potential off-axis according to (1). Indeed, at any  $z_n$ ,  $\phi_{,zz}$  is discontinuous, so that a  $r^2$  discontinuity in potential arise; this term may be neglected in paraxial approximation.

### Piecewise Quadratic Approximation

To apply the quadratic elements in nonparaxial case, imagine to have matched the potential  $\phi$  and field  $E_z$  on axis at breaking

point  $z_n$  between two element intervals; to fix ideas, let  $z_n = 0$ . The two elements are  $\phi_I = A + Bz + C_I(r^2/2 - z^2/4)$  and  $\phi_{II} = A + Bz + C_{II}(r^2/2 - z^2/4)$ , with  $A$  and  $B$  equal because of matching for  $r = 0$ . Requiring potential continuity  $\phi_I = \phi_{II}$  implies

$$r = \sqrt{2}(z - z_n) \quad \text{or} \quad r = \sqrt{2}(z_n - z) \quad (7)$$

These two lines (in fact cones) are the element boundaries and separate three regions; in region III we may have another element as eq. (1) with a different  $C_{III}$  if desired.

Matching  $\phi_{,z}$  off-axis is not possible. Discontinuity of  $E_z$  is equivalent to a charge (say positive), which implies a balancing charge (negative) to be located at lines (7). More quantitatively,  $\Phi_t$  be the true potential ( $\mathbf{E}_t$  the true field),  $\phi$  our collection of elements (so that  $\mathbf{E} = -\text{grad}\phi$  is a part of the electric field) and  $\Phi_c = \Phi_t - \phi$  the correction (localized near eq. (7) lines) that restores matching between elements. From Laplace eq.  $\Delta\Phi_t = 0$  we indeed get:

$$\Delta\Phi_c = \text{div}\mathbf{E} \quad (8)$$

From eq. (7), boundaries associated to different  $z_n$  may intersect at  $r = (z_n - z_{i+1})/\sqrt{2}$ , which determines the maximum radius of validity of our element decomposition.

Non paraxial analysis is more easily applied to the remarkable case of the anode lens [4], a hole of radius  $R$  in a conducting metal sheet (at  $\Phi_t = 0$ ) separating a semispace  $z < 0$  with field  $E_z = E_1 \equiv E_s - E_d$  for  $z \rightarrow -\infty$  from a semispace  $z > 0$  with field  $E_z = E_2 \equiv E_s + E_d$  for  $z \rightarrow +\infty$ . Our field elements are explicitly

$$\begin{aligned} \phi_T &= -E_s z + E_d z & \text{for } r - \sqrt{2}z - R_p > 0 > z \\ \phi_V &= -E_s z - E_d z & \text{for } r + \sqrt{2}z - R_p > 0 < z \\ \phi_U &= -E_s z + (E_d/Z_p)(\frac{1}{4}r^2 - \frac{1}{2}z^2 - \frac{1}{2}Z_p^2) \end{aligned} \quad (9)$$

elsewhere, with  $Z_p = R_p/\sqrt{2}$ . Here  $R_p$  is a parameter; breaking points are at  $\pm Z_p$ . Choosing  $R_p = 4\sqrt{2}/\pi$  gives the exact values for  $\phi_U(0, 0)$ , similarly to einzel lens [4].

From (9) we can compute the fictitious charge of (8):

$$\Delta\Phi_c = \frac{3E_d r}{2^{3/2}Z_p} [\delta(z - Z_p + (r/\sqrt{2})) + \delta(z + Z_p - (r/\sqrt{2}))] \quad (10)$$

The effect of  $\Phi_c$  on particle motion can be approximately described by a (small) transverse kick  $\mathbf{K}$  when passing boundaries; for example crossing  $T$ - $U$  boundary gives

$$K_r = -\frac{E_d r_i^2}{2\sqrt{2}Z_p v_i} (1 + 2^{-5/2}\alpha_i - 0.75\alpha_i^2 + O[\alpha_i^3]) \quad (11)$$

where  $r_i, z_i$  are  $r, z$  at the crossing;  $v_i$  is  $v_z$  at this time;  $\alpha_i$  is  $p_r/p_z$  at this time. Component  $K_z$  is such to maintain energy unchanged. This kick does not contribute to linear focusing, but to aberrations.

We can now formulate a fast tracking for the anode lens. For convenience we project initial and final states on  $z = 0$ . The initial motion:

$$r(z) = r_0 + p_0[\sqrt{f + 2(E_s - E_d)z} - \sqrt{f}]/(E_s - E_d) \quad (12)$$

with  $f = 2E - p_0^2$  is therefore parameterized by  $(r_0, p_0)$ , which would be the values of  $(r, p_r)$  at  $z = 0$ , if our particle would propagate in a constant field  $E_z = E_1$  up to there. From (12) and boundary eq.  $r - \sqrt{2}z = Z_p$  crossing values  $r_i, z_i$  can be easily determined. After crossing we have  $p_i \equiv p_r(z_i) = p_0 + K_r$  with the kick (11). Motion follows eq. (2) up to crossing with  $U-V$  boundary, at  $z = z_o$ ;  $z_o$  is determined by

$$z_o = Z_p - \left[ \frac{r_i}{\sqrt{2}} \cos \psi(z_o, z_i) + \frac{p_i}{\sqrt{C}} \sin \psi(z_o, z_i) \right] \quad (13)$$

which can be solved iteratively. A good starting value for  $\psi$  is  $\psi(Z_p, -Z_p) =$

$$\frac{1}{\sqrt{2}} \left[ \text{Arsh} \frac{E_d + E_s}{\sqrt{g + E_d^2 - E_s^2}} - \text{Arsh} \frac{E_s - E_d}{\sqrt{g + E_d^2 - E_s^2}} \right] \quad (14)$$

with  $g = 2H_z^c E_d / Z_p$ . Final value of  $p_r$  is  $p_r(z_o^+) = p_o + K_r$  where the second kick is given by eq. (11), with  $r_i$  replaced by  $r_o$  (and similar replacement for  $z_i$   $p_i$   $\alpha_i$ ).

### Remarks on Programming

As a general remark, programs become more involved with their size; in our opinion, no recipe can guarantee order and clarity (and absence of error). It is then natural to break a program into several parts, mainly a “physics part” [5], where formula as (1)-(14) are coded as plainly as possible, and an “interpreter”, ultimately relating with numbers and graphics; for example, as COSY and FOXY (interpreting COSY to Fortran [5]). Our try in this direction is the use of an external interpreter, at present Mathematica [2]; advantages of this approach are more evident at the beginning (as now), when the physics code is small enough to make errors unlikely; and reformulation is possible.

A Mathematica applicative program (code in brief) consists of definition of transformation of symbols, with possibility of delaying or conditioning their execution: almost any kind of programming style is possible. It is probable that object programming, implemented by “UpSetDelayed” [2], will be a fairly good recipe to order information about the several treated objects: dipoles, regions of einzel lenses or of accelerating tubes, drifts. At present, a traditional style was used: an element is a list, including the element name, kind of approximation used, and parameters. For example, {dipolex, fringe,  $R, \phi, \alpha, \beta, n, D, I_2(\text{in}), I_2(\text{out})$ } represents H.Engel’s model of dipole [4]. Symbols “matrix2” and “matrix3” represent actions on  $(x, p_x)$  phase-space and  $(x, p_x, \delta)$  space respectively. An einzel lens is converted into a sequence of seven lists. A beamline is a list of lists, on which a traditional loop distributes the action of “matrix3”. Operation on lists may be more concisely done with in-built symbols “Thread” and “Map”, in an advanced style. Graphics rendering was very flexible and satisfying. We plan to merge fitting of elements to einzel into some post-processor of Poisson equation numerical solvers.

### Simulation Results

Let  $(V_2, V_3, V_4)$  be the voltages of the three einzel lenses,  $V_1$  be the source voltage and  $-V_p$  be the linac voltage, referenced to

platform. Fig. 3a) was computed for a beam of  $\text{He}^{2+}$ , setting  $V_1 = 9$  kV, (i.e.  $E = eV_1 = 18$  keV),  $V_2 = 3.45$  kV for the first einzel and optimizing  $(V_3, V_4, V_p) = (7, 5.65, 67)$  kV; a  $\delta V_1 = 10$  V perturbation was added. Simulation for  $\text{Ar}^{14+}$  and  $\text{U}^{28+}$  beams proved even better transport, provided that latter voltages (and intermediate waists) are changed:  $(V_3, V_4, V_p) = (0, 0, 99.6)$  kV and  $(0, 6.3, 314)$  kV respectively. Fig 3b) shows that also aberration can be reproduced by PQA, in fairly good agreement with RungeKutta computations.

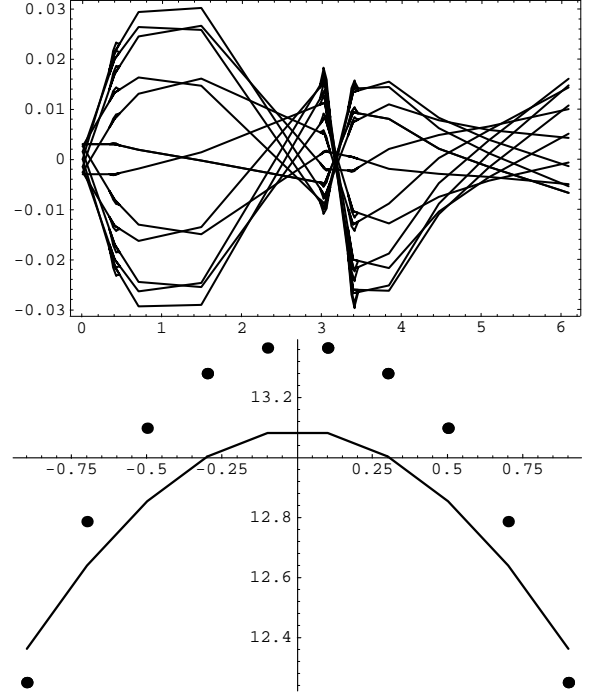


Figure 3: a) Paraxial ray  $r$  versus  $z$  (in m) for the ECR line; 3b) Focal distance  $R$  versus  $r_0/R$  for anode lens (dots: RungeKutta), when  $E_1 = 0$  and  $E_2 = 0.4E/(eR)$ .

### References

- [1] R. Geller, P. Ludwig, G. Melin, *Rev. Sci. Instr.*, 63, 2795 (1992).
- [2] S. Wolfram, *Mathematica*, Addison-Wesley, Redwood City, 1988; Mathematica is a trademark of Wolfram Research Inc.
- [3] P. Grivet, *Electron Optics*, Pergamon, Oxford, 1972, p. 215 (see references to R.J. Rudenberg (1948) and E. Regenstreif (1951a) there) and p. 575ff.
- [4] M.Y. Bernard, p. 14 in *Focusing of charged particles*, (A. Septier, ed.), Academic, Orlando, 1967; also E. Durand, *Electrostatique*, tome II, Masson et C., Paris, 1966; also p. 38 in Ref. [3].
- [5] M. Berz, NIM A298, 473, 1990 and A298, 426, 1990.